



Contents lists available at ScienceDirect

Biochemical and Biophysical Research Communications

journal homepage: [www.elsevier.com/locate/ybbrc](http://www.elsevier.com/locate/ybbrc)



# Direct interaction between EFL1 and SBDS is mediated by an intrinsically disordered insertion domain



Nozomi Asano<sup>a</sup>, Haruka Atsuumi<sup>a</sup>, Akiyoshi Nakamura<sup>b</sup>, Yoshikazu Tanaka<sup>b</sup>, Isao Tanaka<sup>b</sup>, Min Yao<sup>b,\*</sup>

<sup>a</sup> Graduate School of Life Sciences, Hokkaido University, Sapporo 060-0810, Japan

<sup>b</sup> Faculty of Advanced Life Science, Hokkaido University, Sapporo 060-0810, Japan

## ARTICLE INFO

### Article history:

Received 17 December 2013

Available online 7 January 2014

### Keywords:

Ribosome biogenesis

Interaction

Intrinsically disordered protein

Isothermal titration calorimetry

Circular dichroism

## ABSTRACT

Removal of anti-association factor, Tif6 (eIF6), by elongation factor-like 1 (EFL1) and Shwachman–Bodian–Diamond syndrome (SBDS) protein is a critical step in the late stage of ribosome maturation. Although EFL1 is known to have GTPase activity that is stimulated by SBDS, how they cooperatively trigger dissociation of Tif6 from the ribosome remains to be elucidated. In the present study, the interaction between EFL1 and SBDS was analyzed by size exclusion chromatography, gel shift assay, and isothermal titration calorimetry (ITC). The results showed that EFL1 interacted directly with SBDS. ITC experiments using domain-truncated mutants showed that the interaction between EFL1 and SBDS is governed by the insertion domain of EFL1 and domains II–III of SBDS. Circular dichroism spectroscopy showed that the insertion domain of EFL1 has a random structure in the absence of SBDS, whereas the disadvantageous entropy change observed on ITC suggested a fixed conformation coupled with complex formation with SBDS. Based on these observations together with those reported previously, we propose roles of EFL1 and SBDS in ribosomal maturation.

© 2014 Elsevier Inc. All rights reserved.

## 1. Introduction

Shwachman–Diamond syndrome is an autosomal recessive disorder characterized by hematological dysfunction, pancreatic exocrine insufficiency, skeletal abnormalities, and short stature [1]. Approximately 90% of Shwachman–Diamond syndrome cases are caused by mutations in the Shwachman–Bodian–Diamond syndrome (SBDS) gene [2], which encodes a protein of approximately 250 amino acid residues. Orthologs of SBDS have been found in archaea, plants, and other eukaryotes. High-throughput affinity-capture mass spectrometry experiments identified potential interactions between SBDS and ribosome biogenesis factors [3], one of which was GTPase elongation factor-like 1 (EFL1). Genetic studies in *Saccharomyces cerevisiae* indicated that SBDS and EFL1 function cooperatively in a pathway to release the essential nucleolar factor, Tif6, from the late cytoplasmic pre-60S ribosomal subunit [4]. The removal of Tif6—the yeast homolog of mammalian eukaryotic translation initiation factor 6 (eIF6)—is critical for late cytoplasmic maturation of the 60S ribosomal subunit [5]. Tif6 acts as a ribosomal anti-association factor, which binds to the pre-60S subunit to inhibit subunit joining by steric hindrance [6–8]. Therefore, dissociation of Tif6 from pre-60S ribosome is essential for enabling assembly into the 80S subunit.

Biochemical analysis showed that 60S-ribosome dependent GTP hydrolysis of EFL1 was stimulated by SBDS, and SBDS and EFL1 directly catalyzed Tif6 removal by a mechanism that required hydrolysis of GTP by EFL1 [9]. However, it remains to be elucidated how EFL1 and SBDS cooperatively trigger dissociation of Tif6 from the ribosome.

SBDS is composed of three domains (Supplementary Fig. S1), and missense mutations of SBDS associated with Shwachman–Diamond syndrome were identified in all three domains [8]. Nuclear magnetic resonance (NMR) spectroscopy identified domain I of SBDS as an RNA binding site [10]. Moreover, it was reported that two mutants in domain II (R126T and K151N in human) were defective in triggering Tif6 release [9]. However, the roles of domains II and III were unclear. On the other hand, EFL1 shares 26.8% sequence identity with translation elongation factor 2 (EF2), and these two proteins share a ribosome binding site [11]. EFL1 triggers release of Tif6 from the pre-60S ribosome, whereas EF2 assists in the translocation of tRNA and mRNA from the A-site to the P-site of the ribosome. There is a marked difference in domain composition between these proteins, i.e., insertion of an extra ~150-residue domain in EFL1. EFL1 and EF2 are commonly composed of domains G, G', and II–V, but only EFL1 has the insertion region within domain II (Fig. S2) [12]. Although the insertion domain is expected to be an important determinant of the function, the details are still unclear.

\* Corresponding author. Fax: +81 11 706 4905.

E-mail address: [yao@castor.sci.hokudai.ac.jp](mailto:yao@castor.sci.hokudai.ac.jp) (M. Yao).

Here, we performed interaction analysis of EFL1 and SBDS. The results showed that EFL1 binds directly with SBDS, in which the insertion region of EFL1 and domain II–III of SBDS dominate the interaction. The results of spectroscopic analysis taken together with the thermodynamic properties suggested conformational changes in the insertion region of EFL1 coupled with the interaction. Based on these observations, we discuss the significance of the interaction between EFL1 and SBDS for Tif6 removal.

## 2. Materials and methods

### 2.1. Plasmid construction

The gene encoding EFL1 was amplified by PCR from *S. cerevisiae* genomic DNA using the primers EFL1-S-1 and EFL1-AS-1 (Supplementary Table S1), and inserted into the *Sbf*I–*Asc*I sites of a modified pET26b vector (pECO-H2). In the resultant plasmid, a His-tag was attached to the N-terminus of the EFL1 gene. The plasmid for EFL1- $\Delta$ Ins (deletion mutant of the insertion region encoding residues 418–577) was constructed by the inverse PCR method using the EFL1 expression vector as the template and primers EFL1-S-2 and EFL1-AS-2. The DNA fragment for the insertion domain of EFL1 (EFL1-Ins; encoding residues 419–577) was amplified using the primers EFL1-S3 and EFL1-AS-3, followed by insertion into the *Sbf*I–*Asc*I sites of a modified pET26b vector (pECO-GH1). In the resultant plasmid, a GST-tag followed by a TEV protease site and a His-tag were fused at the N-terminus and C-terminus, respectively.

The gene encoding SBDS was amplified by PCR from *S. cerevisiae* genomic DNA using the primers SBDS-S-4 and SBDS-AS-4, and inserted into the *Nde*I–*Xho*I sites of a modified pET28b vector (pDBHT-2), in which a His-tag was fused at the N-terminus. The coding sequences of SBDS domain I (encoding residues 1–94), domain II (encoding residues 95–172), domain III (encoding residues 173–250), domain I–II (encoding residues 1–172), and domain II–III (encoding residues 95–250) were amplified separately by PCR with the expression vector of SBDS as the template and the primers shown in Supplementary Tables S1 and S2. The amplified DNA fragments encoding domains I, II, and I–II were inserted into the *Nde*I–*Xho*I sites of a modified pET28b vector (pET28M), in which His-tag was fused at the N-terminus. The DNA fragments encoding domain III and II–III were inserted into the *Nde*I–*Xho*I sites of the pET26b vector, in which His-tag was attached to the C-terminus.

### 2.2. Protein expression and purification

*Escherichia coli* strain B834 (DE3) harboring the expression vector and pRARE2 was grown at 37 °C in LB medium supplemented with 25  $\mu$ g/mL kanamycin and 34  $\mu$ g/mL chloramphenicol until the OD<sub>600</sub> reached 0.6. To induce expression of the desired protein, IPTG was added at a final concentration of 0.25 mM. After incubation at 25 °C for a further 18 h (exceptionally, for the expression of EFL1, 15 °C for 24 h), cells were harvested by centrifugation at 4500 $\times$ g for 10 min at 4 °C. Cells expressing EFL1 and the mutants were resuspended in 50 mM Tris–HCl (pH 7.5), 300 mM NaCl, 1 mM MgCl<sub>2</sub>, 10% (v/v) glycerol, 1 mg/mL lysozyme, and 0.1 mg/mL DNase I. Cells expressing SBDS and the mutants were resuspended in 50 mM Tris–HCl (pH 7.5), 300 mM NaCl, 10% (v/v) glycerol, 1 mg/mL lysozyme, 0.1 mg/mL DNase I, and 0.1 mg/mL RNase A. Resuspended cells were disrupted by sonication, followed by centrifugation at 40,000 $\times$ g for 1 h at 10 °C.

EFL1 and EFL1- $\Delta$ Ins were purified on a HisTrap HP column (GE Healthcare) and HiLoad 16/60 Superdex 200-pg column (GE Healthcare). EFL1-Ins was purified on a HisTrap HP column (GE Healthcare), followed by removal of the GST-tag by digestion

with TEV protease. EFL1-Ins without the GST-tag was further purified on a HisTrap HP column and HiLoad 16/60 Superdex 200-pg column.

SBDS and its truncated mutants were purified on a HisTrap HP column and HiLoad 26/60 Superdex 75-pg column. Exceptionally, SBDS-domain I was purified by three steps using a HisTrap HP column, HiTrap Heparin HP column, and HiLoad 26/60 Superdex 75-pg column.

### 2.3. Gel filtration analyses

Aliquots of 150  $\mu$ L consisting of 2.5 nmol EFL1 and 8.5 nmol SBDS were loaded onto a HiLoad 10/300 Superdex 200-pg column (GE Healthcare) pre-equilibrated with 20 mM Tris–HCl (pH 7.5), 150 mM NaCl, 1 mM MgCl<sub>2</sub>, 5% (v/v) glycerol, and 5 mM  $\beta$ -mercaptoethanol. Control experiments using each protein were also performed under the same conditions. Peak fractions were analyzed by SDS–PAGE, followed by staining with Coomassie brilliant blue R-250.

### 2.4. Gel shift assay

Gel shift assay was performed in 5- $\mu$ L reaction mixtures containing 20 mM Tris–HCl (pH 7.5), 150 mM NaCl, 1 mM MgCl<sub>2</sub>, 5% (v/v) glycerol, 5 mM  $\beta$ -mercaptoethanol, and the desired amounts of EFL1 and SBDS. Reaction mixtures were loaded onto a 3–10% native gradient polyacrylamide gel (PAGE L NPG-310L; ATTO). Electrophoresis conditions were as follows: temperature, 4 °C; power voltage, 100 V; and electrophoresis buffer, 50 mM Tris–MES (pH 8.0) and 10 mM Mg (OAc)<sub>2</sub>. Proteins were visualized using SYPRO® Ruby Protein gel stain.

### 2.5. Isothermal titration calorimetry

All isothermal titration calorimetry (ITC) measurements were carried out with a VP-ITC System (MicroCal). Proteins were dialyzed against a buffer containing 20 mM Tris–HCl (pH 7.5), 150 mM NaCl, 1 mM MgCl<sub>2</sub>, 10% (v/v) glycerol, and 5 mM  $\beta$ -mercaptoethanol at 4 °C. All measurements were conducted at 30 °C and protein solutions were degassed under vacuum prior to use. The cell was filled with  $\sim$ 5  $\mu$ M full-length EFL1, EFL1- $\Delta$ Ins or  $\sim$ 2.5  $\mu$ M EFL1-Ins, and a syringe was filled with  $\sim$ 50  $\mu$ M full-length SBDS or each truncated SBDS. The solution of SBDS was injected 25 times in portions of 10  $\mu$ L over 20 s. The data were analyzed using the program ORIGIN (MicroCal).

### 2.6. Circular dichroism measurements

Circular dichroism (CD) spectra were measured on a JASCO J-720 spectropolarimeter (JASCO) in a quartz cell with an optical path length of 2 mm. The CD spectra were obtained by taking the average of four scans made from 300 to 190 nm and normalized to molar ellipticities by protein concentrations.

### 2.7. Model building of EFL1-Tif6-bound ribosome

The binding position of Tif6 on EF2-60S complex was obtained by superposing 60S ribosome subunits of eIF6(Tif6)-60S (PDB code: 4A18 [13]) and EF2-60S complex structure (PDB code: 1S1H and 1S1I [14]) using the program PyMol (The PyMOL Molecular Graphics System, Schrödinger, LLC, New York, NY). The final model of the EFL1-Tif6-bound 60S ribosome subunit was built by superposing the crystal structure of Tif6 (PDB code: 1G62 [6]) onto the Tif6-EF2-60S model [15].

### 3. Results

#### 3.1. Interaction between EFL1 and SBDS

To investigate the details of the interaction between EFL1 and SBDS, the binding of EFL1 with SBDS was analyzed by size exclusion chromatography (SEC), gel shift assay, and isothermal titration calorimetry (ITC). Fig. 1A shows the results of SEC. Compared with EFL1 and SBDS eluted with peaks at 11.19 and 15.15 mL, respectively, the mixture showed a slightly earlier peak at 11.11 mL. SDS-PAGE showed that both EFL1 and SBDS were contained in the peak of mixed sample (Fig. 1B), indicating the direct interaction between EFL1 and SBDS. Gel shift assay also clearly showed the interaction between EFL1 and SBDS (Fig. 1C). With increasing concentration of SBDS, the migration speed of EFL1 was significantly slowed. As EFL1 has GTPase activity, these experiments were also performed in the presence of GDPNP (an analog of GTP). However, there were no significant differences from the results in the absence of GTP (Fig. 1A). These results indicated that EFL1 and SBDS directly interact with each other in a GTP-independent manner. Next, we determined the thermodynamic parameters of the interaction by ITC (Fig. 1C and Table 1). The association constant and stoichiometry were  $12.7 \times 10^6 \text{ M}^{-1}$  and 0.94, respectively, indicating that EFL1 binds to SBDS with a molar ratio of 1:1. The binding

enthalpy, entropy, and Gibbs's energy were calculated to be  $-14.0 \text{ kcal mol}^{-1}$ ,  $-13.5 \text{ cal mol}^{-1} \text{ K}^{-1}$ , and  $-9.86 \text{ kcal mol}^{-1}$ , respectively, indicating that the interaction between EFL1 and SBDS is driven by enthalpy and is entropically disadvantageous.

#### 3.2. Identification of the binding region in EFL1

EFL1 shares sequence similarity with translation elongation factors, EF-G and EF-2 (Fig. 2A and Supplementary Fig. S2). These proteins commonly consist of the G domain (domain I), which binds with and hydrolyzes GTP, the G' domain, and domains II to V (Fig. S2). On the other hand, EFL1 has a characteristic insertion domain of 160 amino acids within domain II. To clarify the contribution of the insertion domain to the interaction with SBDS, the insertion domain of EFL1 (EFL1-Ins; Gly<sup>419</sup>-Glu<sup>577</sup>) and a mutant protein in which the insertion domain was deleted (EFL1-ΔIns) were prepared, and their affinities with SBDS were evaluated by ITC (Fig. 2B). EFL1-Ins bound with SBDS, whereas no significant interaction was observed for EFL1-ΔIns. The association constant,  $11.8 \times 10^6 \text{ M}^{-1}$  of EFL1-Ins, did not decrease markedly compared with that of EFL1 (Table 2). The thermodynamic parameters were binding enthalpy of  $-16.7 \text{ kcal mol}^{-1}$  and binding entropy of  $-22.8 \text{ cal mol}^{-1} \text{ K}^{-1}$ , indicating that EFL1-Ins binds to SBDS in an enthalpy-driven manner, which was the same as that of EFL1.

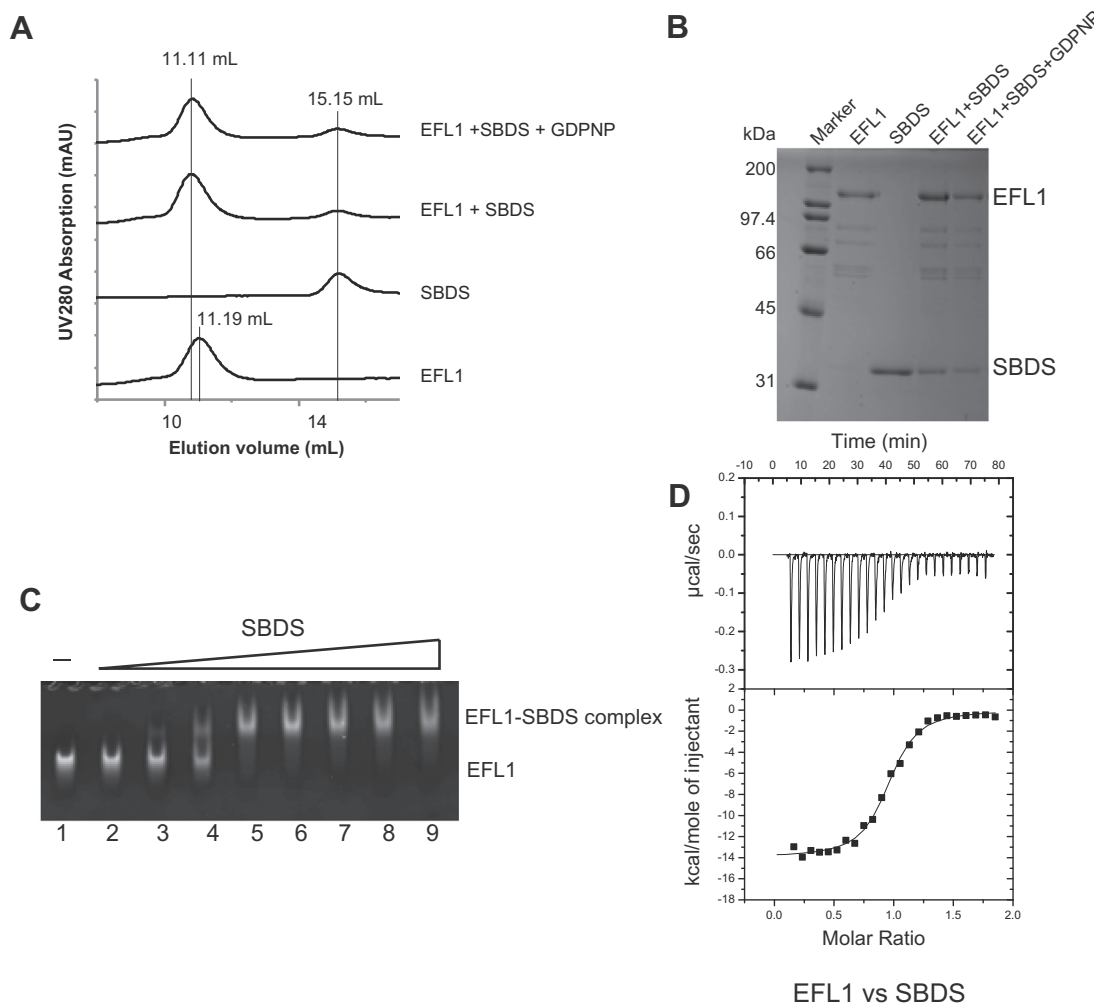


**Fig. 1.** Interaction between EFL1 and SBDS. (A) Size exclusion chromatography of EFL1 incubated with SBDS. Chromatograms of EFL1, SBDS, and their complex in the presence of GDPNP are also shown. The elution volumes are indicated at the tops of the peaks. (B) SDS-PAGE of the peak fractions on size exclusion chromatography. Lane 1, EFL1; lane 2, SBDS; lane 3, EFL1-SBDS; lane 4, EFL1-SBDS in the presence of GDPNP. (C) Results of gel shift assay. A 50-pmol aliquot of EFL1 was incubated with different amounts of SBDS. Lane 1, EFL1 only; lanes 2–8, increasing amounts of SBDS (2, 5, 10, 25, 50, 100, 500, 1000 pmol). (D) Thermogram of interaction between EFL1 and SBDS.

**Table 1**  
Affinity and thermodynamic parameters of binding between SBDS and EFL1 at 30 °C.

EFL1	SBDS	N	$K_b (\times 10^6 \text{ M}^{-1})$	$K_d^a (\text{nM})$	$\Delta H (\text{kcal mol}^{-1})$	$\Delta S (\text{cal mol}^{-1} \text{ K}^{-1})$	$\Delta G^b (\text{kcal mol}^{-1})$
Full length	Full length	$0.94 \pm 0.007$	$12.7 \pm 1.51$	78.7	$-14.0 \pm 0.17$	-13.5	-9.86

<sup>a</sup>  $K_d = 1/K_b$ .  
<sup>b</sup>  $\Delta G = -RT \ln K_b = \Delta H - T\Delta S$ .

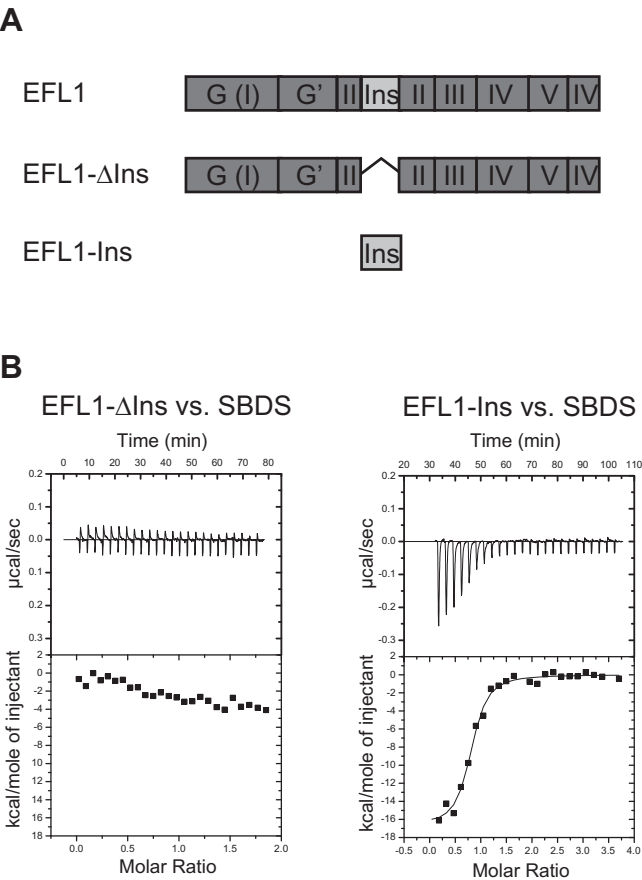


**Fig. 2.** Interaction of EFL1 mutants for SBDS. (A) Schematic overview of the EFL1 variants. The insertion sequence within domain II is shown in light gray. (B) Thermograms of titration for SBDS of EFL1-ΔIns (left) and EFL1-Ins (right).

Furthermore, EFL1 and EFL1ΔIns showed similar circular dichroism (CD) spectra, suggesting that truncation of the insertion domain did not affect the folding of EFL1 (Fig. 3). These observations indicated that the insertion region of EFL1 plays a pivotal role in the interaction with SBDS. The CD spectrum of EFL1-Ins showed a weak negative peak around 220 nm and strong negative CD around 200 nm (Fig. 3). These spectral features indicated that the insertion domain has a random structure with a small quantity of β-strands.

3.3. Identification of the binding region in SBDS

It has been reported that SBDS is composed of three domains with weak contacts among them [8–10]. As SBDS family proteins

**Table 2**  
Affinities and thermodynamic parameters of binding between SBDS and EFL1 mutants at 30 °C.

EFL1	SBDS	N	$K_b (\times 10^6 \text{ M}^{-1})$	$K_d (\text{nM})$	$\Delta H (\text{kcal mol}^{-1})$	$\Delta S (\text{cal mol}^{-1} \text{ K}^{-1})$	$\Delta G (\text{kcal mol}^{-1})$
ΔIns	Full length	ND <sup>a</sup>	ND	ND	ND	ND	ND
Ins	Full length	$0.778 \pm 0.02$	$11.8 \pm 2.45$	84.7	$-16.7 \pm 0.51$	-22.8	-9.81

<sup>a</sup> ND: not detected.

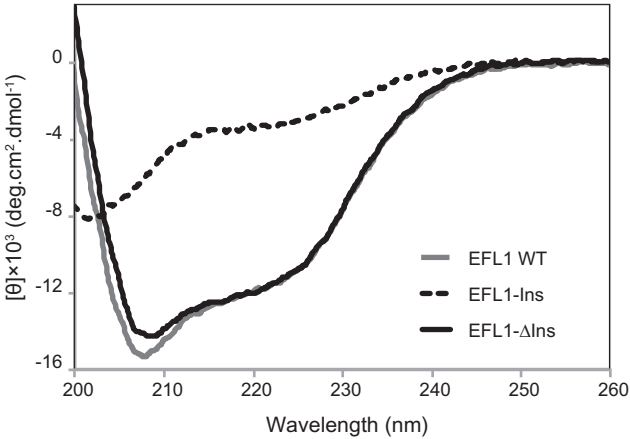


**Fig. 3.** CD spectra of EFL1 variants. Gray line; EFL1 wild type, black line; EFL1-ΔIns, dotted black line; EFL1-Ins.

share a similar structure and sequence, ScSBDS is expected to consist of domain I (Met1–Gln94), domain II (Leu95–Ala172), and domain III (Lys173–Asn250) (Fig. S1). Therefore, we prepared five domain-truncated mutants of SBDS (SBDS I, SBDS II, SBDS III, SBDS I–II, and SBDS II–III), and their interactions with EFL1 were evaluated by ITC (Fig. 4 and Table 3).

SBDS II–III showed significant interaction with EFL1, whereas domain I–II did not (Fig. 4A and B). The association constant of SBDS II–III with EFL1 was determined to  $1.19 \times 10^6 \text{ M}^{-1}$ . The thermodynamic parameters indicated an enthalpy-driven and entropically disadvantageous interaction as observed in the interaction between intact SBDS and EFL1. Despite the observations in SBDS II–III, none of the other SBDS mutants showed significant interactions with EFL1 by themselves. These results indicated that both domains II and III of SBDS contribute to the interaction with EFL1. Taken together, these results indicated that the insertion domain of EFL1 and both domains II and III of SBDS dominate the enthalpy-driven entropically disadvantageous interaction between EFL1 and SBDS.

4. Discussion

4.1. Biological implications of SBDS–EFL1 interaction

Both SBDS and EFL1 were bound with the ribosome by itself [9]. It has been reported that EFL1 binds at the same site the on ribosome as EF2 [11], whereas the site for SBDS binding has not yet been identified. Our results showed that EFL1 interacted with SBDS directly, and this is the first study demonstrating the detailed

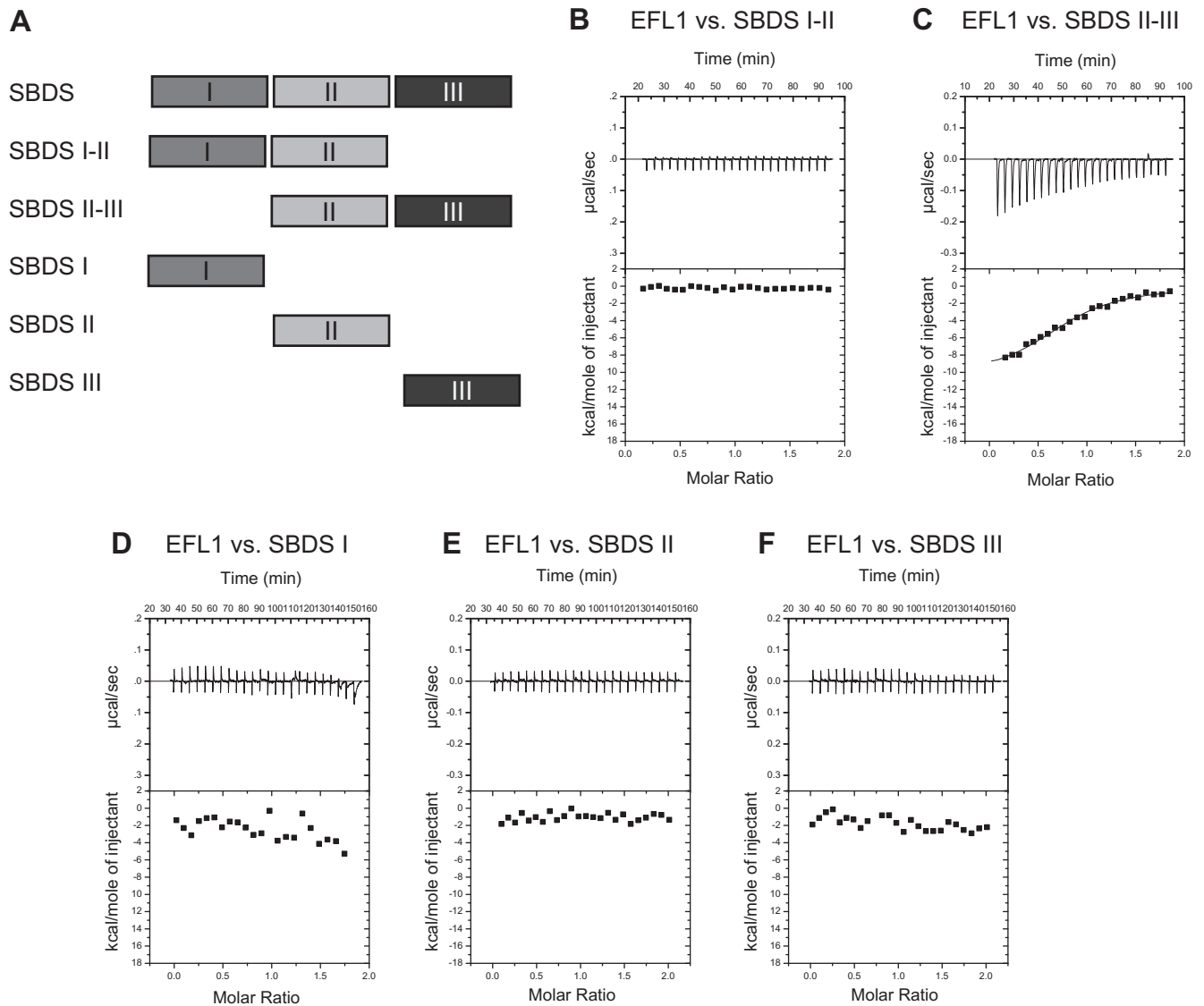


**Fig. 4.** Interaction of SBDS mutants for EFL1. (A) Schematic overview of the SBDS variants. (B–F) Thermograms of titration of SBDS variants for EFL1. B; SBDS I–II, C; SBDS II–III, D; SBDS I, E; SBDS II, F; SBDS III.

**Table 3**

Affinities and thermodynamic parameters of binding between SBDS mutants and EFL1 at 30 °C.

EFL1	SBDS	N	$K_b$ ( $\times 10^6 \text{ M}^{-1}$ )	$K_d$ (nM)	$\Delta H$ (kcal mol $^{-1}$ )	$\Delta S$ (cal mol $^{-1} \text{ K}^{-1}$ )	$\Delta G$ (kcal mol $^{-1}$ )
Full length	I–II	ND <sup>a</sup>	ND	ND	ND	ND	ND
Full length	II–III	$0.803 \pm 0.03$	$1.19 \pm 1.69$	840	$-10.6 \pm 0.52$	-7.04	-8.43
Full length	I	ND	ND	ND	ND	ND	ND
Full length	II	ND	ND	ND	ND	ND	ND
Full length	III	ND	ND	ND	ND	ND	ND

<sup>a</sup> ND: not detected.

interaction between them. The direct interaction indicated that SBDS binds in the vicinity of the EF2/EFL1 binding site on the ribosome. Oliveira et al. demonstrated that SBDS interacted with ribosomal RNA via domain I [10]. In addition, Finch et al. showed that the motion of domain I of SBDS was independent of domain II–III [9]. Our results demonstrated a significant role of domain II–III of SBDS in the interaction with EFL1. Taken together, these results suggest that domains I and II–III of SBDS are likely to act as functionally independent domains; i.e., domain I and domain II–III bind to the ribosome and EFL1, respectively. EFL1 competes with EF2

for binding at the ribosomal GTPase binding site. This site will be occupied by EFL1 during ribosome biogenesis, whereas EF2 binds there in the elongation step during translation. The interaction between SBDS and EFL1 may facilitate predominant recruitment of EFL1 in the final maturation process of ribosome biogenesis.

To discuss the significance of the SBDS–EFL1 interaction in release of Tif6, a structural model of Tif6–EFL1–60S complex was constructed from the crystal structures of Tif6–60S complex and EF2–60S complex (Supplementary Fig. S3). In the model, EFL1 is



positioned adjacent to Tif6, in which domain II of EFL1 is expected to show extensive interactions with Tif6. The insertion domain of EFL1, which is located within domain II, is necessary for the interaction with SBDS. Therefore, the insertion domain is likely to be toward Tif6. As the insertion domain is recognized by SBDS, the binding site of SBDS on the ribosome is expected to be close to the Tif6 binding site. Taken together, it is plausible that both EFL1 and SBDS are positioned in close proximity to Tif6 on the ribosome. However, the results of size exclusion chromatography indicated that Tif6 interacts with neither EFL1 nor SBDS directly (Supplementary Fig. S4). Biochemical analyses demonstrated that the presence of both EFL1 and SBDS, and GTP hydrolysis of EFL1 are all essential for the release of Tif6. Moreover, the presence of SBDS enhances the GTPase activity of EFL1 [9,16]. SBDS may increase the GTPase activity of EFL1 through complex formation. This is supported by the report that substitution in the domain II–III of SBDS resulted in a significant decrease in GTPase activity of EFL1 [9]. The GTPase activity would induce a conformational change of EFL1 as observed from other translational factors possessing GTPase activity, e.g., EF2 [12,17]. As Tif6 did not interact with EFL1 directly (Supplementary Fig. S3), the conformational change of EFL1 is likely to trigger release of Tif6 indirectly. As reported for EF2, the conformational change of EFL1 may induce rearrangement of the ribosome, which may result in the release of Tif6. These are consistent with the mechanism proposed previously [4].

#### 4.2. Role of the insertion domain of EFL1

Although EFL1 and EF2 bind to the identical site on the ribosome, they have different functions [11]. They are clearly distinguished each other by the presence or absence of an insertion sequence within domain II. The CD spectra showed that the insertion domain of EFL1 (EFL1-Ins) was a random structure. On the other hand, ITC experiments showed that the interaction between EFL1 and SBDS was entropically disadvantageous. These observations indicate that the random structure of the insertion domain of EFL1 became static upon SBDS binding. It is likely that the insertion domain acts as an intrinsically disordered protein. Similar structural transition from a flexible to a rigid form coupled with ligand binding was reported previously for initiation factors [18]. The GTPase activity of EFL1 necessary for Tif6 release is enhanced by the presence of SBDS [9]. Our results indicated a direct interaction of the insertion domain of EFL1 with SBDS accompanying conformational transition. These observations suggest that the fixed conformation is important for the release of Tif6. EFL1 may be necessary to acquire the intrinsically disordered domain as an insertion domain to express these two different functions, i.e., inhibition of EF2-like activity utilizing the unfolded structure and promoting Tif6 release in the fixed form.

#### Acknowledgment

This work was supported by Grant-in-aid for Scientific Research (B) (No. 25291008 to M. Y.) from the Ministry of Education, Culture, Sports, Science and Technology of Japan.

#### Appendix A. Supplementary data

Supplementary data associated with this article can be found, in the online version, at <http://dx.doi.org/10.1016/j.bbrc.2013.12.143>.

#### References

- [1] G.W. Hall, P. Dale, J.A. Dodge, Shwachman-Diamond syndrome: UK perspective, *Arch. Dis. Child.* 91 (2006) 521–524.
- [2] G. Horiguchi, H. Kodama, K. Iba, Mutations in a gene for plastid ribosomal protein S6-like protein reveal a novel developmental process required for the correct organization of lateral root meristem in Arabidopsis, *Plant J.* 33 (2003) 521–529.
- [3] N.J. Krogan, G. Cagney, H. Yu, G. Zhong, X. Guo, A. Ignatchenko, J. Li, S. Pu, N. Datta, A.P. Tikuisis, T. Punna, J.M. Peregrin-Alvarez, M. Shales, X. Zhang, M. Davey, M.D. Robinson, A. Paccanaro, J.E. Bray, A. Sheung, B. Beattie, D.P. Richards, V. Canadien, A. Lalev, F. Mena, P. Wong, A. Starostine, M.M. Canete, J. Vlasblom, S. Wu, C. Orsi, S.R. Collins, S. Chandran, R. Haw, J.J. Rillstone, K. Gandi, N.J. Thompson, G. Musso, P. St Onge, S. Ghanny, M.H. Lam, G. Butland, A.M. Altaf-Ul, S. Kanaya, A. Shilatifard, E. O'Shea, J.S. Weissman, C.J. Ingles, T.R. Hughes, J. Parkinson, M. Gerstein, S.J. Wodak, A. Emili, J.F. Greenblatt, Global landscape of protein complexes in the yeast *Saccharomyces cerevisiae*, *Nature* 440 (2006) 637–643.
- [4] T.F. Menne, B. Goyenechea, N. Sanchez-Puig, C.C. Wong, L.M. Tonkin, P.J. Ancliff, R.L. Brost, M. Costanzo, C. Boone, A.J. Warren, The Shwachman-Bodian-Diamond syndrome protein mediates translational activation of ribosomes in yeast, *Nat. Genet.* 39 (2007) 486–495.
- [5] U. Basu, K. Si, J.R. Warner, U. Maitra, The *Saccharomyces cerevisiae* TIF6 gene encoding translation initiation factor 6 is required for 60S ribosomal subunit biogenesis, *Mol. Cell. Biol.* 21 (2001) 1453–1462.
- [6] C.M. Groft, R. Beckmann, A. Sali, S.K. Burley, Crystal structures of ribosome anti-association factor IF6, *Nat. Struct. Biol.* 7 (2000) 1156–1164.
- [7] M. Ceci, C. Gaviarighi, C. Gorrini, L.A. Sala, N. Offenhauser, P.C. Marchisio, S. Biffo, Release of eIF6 (p27BBP) from the 60S subunit allows 80S ribosome assembly, *Nature* 426 (2003) 579–584.
- [8] C. Shammas, T.F. Menne, C. Hilcenko, S.R. Michell, B. Goyenechea, G.R. Boock, P.R. Durie, J.M. Rommens, A.J. Warren, Structural and mutational analysis of the SBDS protein family. Insight into the leukemia-associated Shwachman-Diamond Syndrome, *J. Biol. Chem.* 280 (2005) 19221–19229.
- [9] A.J. Finch, C. Hilcenko, N. Basse, L.F. Drynan, B. Goyenechea, T.F. Menne, A. Gonzalez Fernandez, P. Simpson, C.S. D'Santos, M.J. Arends, J. Donadieu, C. Bellanne-Chantelot, M. Costanzo, C. Boone, A.N. McKenzie, S.M. Freund, A.J. Warren, Uncoupling of GTP hydrolysis from eIF6 release on the ribosome causes Shwachman-Diamond syndrome, *Genes Dev.* 25 (2011) 917–929.
- [10] J.F. de Oliveira, M.L. Sforza, T.M. Blumenschein, M.B. Goldfeder, B.G. Guimaraes, C.C. Oliveira, N.I. Zanchin, A.C. Zeri, Structure, dynamics, and RNA interaction analysis of the human SBDS protein, *J. Mol. Biol.* 396 (2010) 1053–1069.
- [11] J.S. Graindorge, J.C. Rousselle, B. Senger, P. Lenormand, A. Namane, F. Lacroute, F. Fasiolo, Deletion of EFL1 results in heterogeneity of the 60 S GTPase-associated rRNA conformation, *J. Mol. Biol.* 352 (2005) 355–369.
- [12] R. Jorgensen, P.A. Ortiz, A. Carr-Schmid, P. Nissen, T.G. Kinzy, G.R. Andersen, Two crystal structures demonstrate large conformational changes in the eukaryotic ribosomal translocase, *Nat. Struct. Biol.* 10 (2003) 379–385.
- [13] S. Klinge, F. Voigts-Hoffmann, M. Leibundgut, S. Arpagaus, N. Ban, Crystal structure of the eukaryotic 60S ribosomal subunit in complex with initiation factor 6, *Science* 334 (2011) 941–948.
- [14] C.M. Spahn, M.G. Gomez-Lorenzo, R.A. Grassucci, R. Jorgensen, G.R. Andersen, R. Beckmann, P.A. Penczek, J.P. Ballesta, J. Frank, Domain movements of elongation factor eEF2 and the eukaryotic 80S ribosome facilitate tRNA translocation, *EMBO J.* 23 (2004) 1008–1019.
- [15] M. Gartmann, M. Blau, J.P. Armache, T. Mielke, M. Topf, R. Beckmann, Mechanism of eIF6-mediated inhibition of ribosomal subunit joining, *J. Biol. Chem.* 285 (2010) 14848–14851.
- [16] A. Gijssbers, A. Garcia-Marquez, A. Luviano, N. Sanchez-Puig, Guanine nucleotide exchange in the ribosomal GTPase EFL1 is modulated by the protein mutated in the Shwachman-Diamond Syndrome, *Biochem. Biophys. Res. Commun.* 437 (2013) 349–354.
- [17] D.J. Taylor, J. Nilsson, A.R. Merrill, G.R. Andersen, P. Nissen, J. Frank, Structures of modified eEF2 80S ribosome complexes reveal the role of GTP hydrolysis in translocation, *EMBO J.* 26 (2007) 2421–2431.
- [18] Z. Gai, Y. Kitagawa, Y. Tanaka, N. Shimizu, K. Komoda, I. Tanaka, M. Yao, The binding mechanism of eIF2beta with its partner proteins, eIF5 and eIF2Bepsilon, *Biochem. Biophys. Res. Commun.* 423 (2012) 515–519.